Journal of Power and Energy Systems

Vol. 1, No. 3, 2007

Simulation and Feasibility Study on a 'Renewable Energy House' with a Geothermal Heat Pump-Powered Floor Heating System in Cold Climate Regions*

Masafumi SASAKI **, Itoro AKPAN *** and Noboru ENDOH ****

, ** Department of Mechanical Engineering, Kitami Institute of Technology, 165 Koen-cho, Kitami, Hokkaido 090-8507, Japan

*** Solar Silicon Technology Co., Ltd, WTC Chiba Fujimi Building, 2-9-13 Fujimi, Chuo-ku, Chiba, Japan

**E-mail: sasaki-m@mail.kitami-it.ac.jp

Abstract

An actual renewable energy house, equipped with a geothermal heat pump (GHP) -powered floor heating system was investigated and analyzed. Daily annual monitoring between February 2005 ~ February 2006 and real-time continuous system monitoring within selected periods during the winter season between November 2006 ~ January 2007, were carried out in order to establish the actual performance of the system. It emerged that the GHP-powered floor heating system is sufficient for space heating, with the maintenance of near-uniform room temperatures even during the coldest days in a very cold region like Hokkaido, Japan. About 37% average of the floor heat losses are recoverable and more than 50% of the ventilation heat losses are recovered due to various innovative energy-saving techniques built into the system. Annual heat loss from the house estimated by the numerical simulation showed good agreement with the measured annual thermal demand for room heating. The simulation also estimated that annual running costs and Green House Gas (GHG) emissions reductions of 47% and 49% respectively, can be realized with this system compared to an equivalent conventional system. A detailed cost analysis for the GHP-only system revealed that if the cost of fuel oil increases by about 50% from the current value of ¥80/L, then the payback period for a GHP-powered renewable energy system is about 14 years. This payback period reduces to about 10 years if 30% of the initial cost of the GHP-powered system is externally funded.

Key words: Renewable Energy, Floor Heating, Geothermal Heat Pump, Energy Balance, CO_2 Emissions, Cold Climate Regions

1. Introduction

There is growing awareness that renewable energy technologies hold the key to solving the worlds' climate problems and ensuring sustainable energy supply and diversification. The Third Assessment Report of the United Nations' Intergovernmental Panel on Climate Change (IPCC), produced by three working groups [(1)], focused on climate science, adaptation and mitigation and concluded that there is a range of renewable energy options that could be implemented over the next 20 years to help reduce GHG emissions. There is worldwide consensus that ways must be found to reduce GHG emissions and renewable energy is one way through which this goal can be achieved.

Various renewable energy systems are being developed throughout the world for

*Received 16 Aug., 2007 (No. 07-0364)
[DOI: 10.1299/jpes.1.251]

commercial, industrial and domestic use. For household energy uses, the main emphasis has mostly been with photovoltaic (PV) systems for electric power generation, for driving pumps or other household equipment for various uses, or the usage of solar thermal collectors as supplementary heat-generating devices to conventional heaters for hot water production. The authors had developed PV/thermal hybrid collectors to get maximum energy gain from solar radiation [2]. For cold climate regions, however, the use of thermal collectors is severely limited during cold seasons, due to excessive low ambient temperatures and minimal available solar radiation [3],[4]. In these regions, it is increasingly becoming more fashionable to harness and use geothermal energy, which source temperature is more stable and warmer in winter than the ambient temperature, for water heating. The geothermal heat pump (GHP) can be used in a wide variety of ways, from provision of hot water for household use, to the provision of source thermal energy to floor heaters for space heating.

The floor heating system has several advantages over conventional forced fan convector systems. The general problem of room air temperature imbalance caused by convective systems has largely been remedied through the use of the floor heater. In addition to minimizing drafts and dusts movements, the floor heating system ensures excellent control of the mean radiant temperature (MRT) for thermal comfort. The MRT refers to the average temperature of all surfaces in a controlled enclosure [5]. Significant works on the 2-D and 3-D modeling of the floor heating systems have already been reported [6-9].

In the previous work we proposed a very simple and highly accurate numerical simulation method which estimated annual energy balances of a renewable energy system with GHP and solar PV/thermal collectors [3]. Annual running costs and CO_2 emissions in several renewable energy systems including a GHP were evaluated using the simulation method and the optimum systems were proposed [4]. In this work, a renewable energy "Model House", situated in Kitami city, on the north-eastern part of Hokkaido, is examined and reported. It is an actual GHP powered house, built by a building company in Kitami mainly for the purpose of feasibility studies. The measured annual thermal demand for room heating is compared with the annual heat loss predicted by the simplified simulation method proposed in the previous works. Real time measurements and simulations are also carried out in order to evaluate the overall transient characteristics of a GHP/house system. Finally, a cost analysis of the GHP-powered heating system, based on current market economies in Japan, including initial and running costs is also presented to highlight the prospects and limitations of realizing domestic-size renewable energy systems especially in very cold climate regions like Kitami city.

2. Geothermal Heat Pump (GHP) System with Floor Heating

A schematic of a geothermal heat pump (GHP) system in the 'Model House' is shown in Figure 1(a) while Fig. 1(b) shows the exterior view of the house that is equipped with the floor heating system. The floor heaters are located both at the first floor (*1F*) and the second floor (*2F*) of the building. In the *1F*, the floor heating system consists of a 70mm concrete slab with embedded heating tubes. The PVC (polyvinyl chloride) tubes embedded in the concrete slab are spaced 182mm apart and the outer diameter of the tubes is 13mm. The total floor area of the 1F floor is 53.9m^2 while the floor of the 2F is 43.9m^2 but the available floor areas for room heating are 31.2m^2 for the *1F* and 22.4m^2 for the *2F* respectively. During the heating season, hot brine (propylene glycol) from the geothermal heat pump condenser, is led through the heating tubes embedded in the concrete slab for room heating. The inlet floor temperature of the brine is controlled according to the time-dependent heating demand of the building envelope through an inverter-control unit.

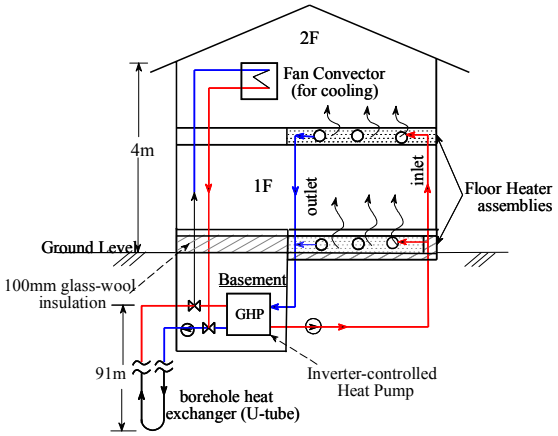

(a) Schematic

(b) Exterior view

Fig. 1 Renewable energy system with a GHP-powered floor heating

The average room temperature during the heating seasons (winter, spring and autumn) was maintained between 21°C~23°C and about 25°C during summer. A U-tube was laid under the ground at the depth of 91 m and ethylene glycol circulated through the evaporator of the GHP.

The GHP unit (Fig. 2) is located at the basement, which also houses an electric water storage tank for hot water supplies. Table 1 summarizes the specifications of the GHP, which is made in Japan. The model house is also equipped with a 'Pellet Stove', a wood-source heater for supplementary room heating during extremely cold periods when the floor heating system is not operational or may be insufficient for room heating. The Pellet Stove rated power is 8~10kW, with 90% efficiency.

During summer, only the U-tube brine circulated through a fan convector used for cooling with no GHP operation. The cooling performance of the fan convector is about 2.5 kW when the room temperature is 26 ℃ at the brine inlet temperature of 8 ℃. The fan is driven by a 40 W electric motor.

Fig. 2 GHP unit installed at the basement

Table 1 Specifications of the GHP Unit

Maker		SUNPOT (Japan)
Rated Power (kW)	Compressor	1.5
	Circulation Pumps	0.22
Refrigerant		R410A
Dimension (cm)		W65*L47*H74
Propylene Glycol Ethylene Glycol		Floor heater side: 4.3L Geothermal tube side: 2.4L

3. Modeling of the 'Model House'

3.1 Heat loss coefficient: Equivalent *Q*-value, Q_{eq}

Recently in cold climate regions, desirable *Q*-value for a 'highly insulated house' is nearly unity (1W/m^{2}K). The *Q*-value is a heat-retention parameter frequently used in Japan to express the insulation level of buildings. An equivalent *Q*-value (Q_{eq}) was estimated by:

$$Q_{eq} = \frac{H_{overall}}{A_{floor}(T_{room} - T_{air})} \quad (1)$$

where $H_{overall}$ (W) denotes the aggregate heat losses/gains from all walls, roof, etc which are estimated by heat transfer models below, where A_{floor} is the total floor area of the house, T_{room} is the average room temperature and T_{air} is the ambient temperature.

3.2 Air Thermal Jacket on the Walls, Floors and Roof

The configuration of the highly-insulated 'Model House' which was observed in present paper is illustrated in detail in Fig. 3. The configuration is essentially so-called 'Outer Insulation Method' in Japan. It consists of the layers (from indoor to outdoor) of inside wall, air-space-and-wood-stud (inner air space), water proof sheathing, thermal insulation board (extruded polystyrene foam), air-space-and-wood-stud (outer air space), and the wall siding. Heat losses from the elevated air temperature stream are reduced by the adjoining and bounding 75mm polystyrene foam insulation. This technique brings about the reduction of the thermal loss gradient from the building interior to the outdoor through the air cavity thereby reducing the overall building thermal losses. The configuration of the frame wall results in a total thermal resistance of about 3.7 m^2K/W for the wall assembly..

Figure 3 also shows the configuration of roof assembly of the model house with the following components: polystyrene foam insulation (125mm), 30mm air space, 12mm wood roof shingles and asphalt zinc. The total thermal resistance for the roof assembly is about 4.2 m^2K/W. Generally, of cause depending on the insulator thickness though, heat losses from walls and roofs are lower in this 'Outer Insulation Method' than those in the conventional configuration which is so-called 'Inner Insulation (or Filling with Insulator) Method'.

The floor heating system (1F) is also shown in Fig. 3. Unusual configuration of an air space was put between the floor covering (floor wood) and the heated concrete slab. Conversely, this air space increases the thermal resistance to room-side heat flux from the heated concrete. These configurations were carefully modeled, so that the value of Q_{eq} for the Model House of 1.09 W/m^2K was estimated.

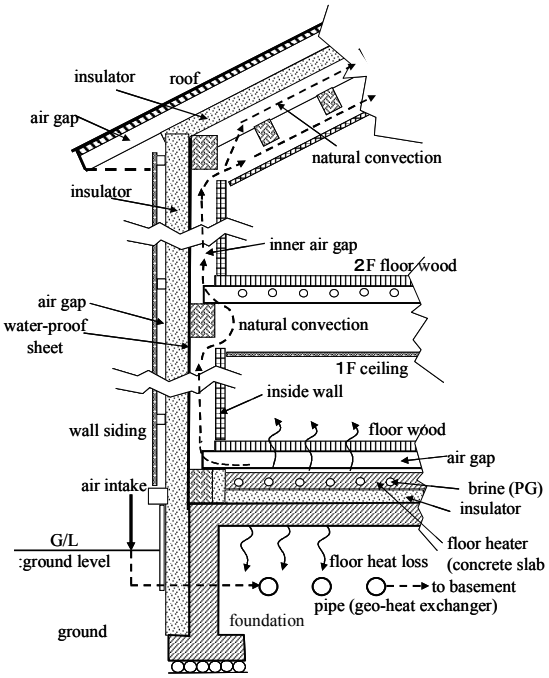

Fig.3 Configuration of the Model House which is constructed with so-called the 'Outer Insulation Method' and with advanced floor heating system.

Since the inner air-space was connected with the floor air space mentioned above, heated air on the concrete slab was delivered through the inner air space to the roof air space by natural convection. The distribution of warm air to walls and roofs, which was forming an air jacket around the building envelope as shown in Fig. 3, made the inside wall temperature higher. The higher wall surface temperatures lead to lower heat loss from the residents to the walls by radiation. This is due to the fact that the operative temperature for required human comfort may be maintained by controlling the mean radiant temperature (MRT) of the conditioned space. As the result, this warm air-jacketed room with floor heating under the room temperature of 20-23 ℃ was sufficiently comfortable, whereas almost all people experience cold feeling in the room heated by a conventional oil heater under the same room temperature.

3.3 Ventilation System: Recovering Floor Heat Loss by Geo-heat exchanger

The new regulation for the ventilation of 0.5 times of house volume/hr was forced in Japan in 2005 to prevent so-called 'Sick House Syndrome' caused mainly by volatile organic compounds (VOCs). The efficient building insulation of the walls, roof and the floor results in a highly sealed building, so that the continuous ventilation becomes more important. The seal performance of a house is expressed with '*C*-value' which is defined as an ratio of equivalent air leakage area (cm^2) to the exterior area (m^2) of the building. The *C*-value of the model house, which was obtained through pressurized measurement technique, was $0.3cm^2/m^2$. Figure 4 show the schematic of the ventilation system and the technique for recovering the downward heat losses from the concrete floor and for avoiding freezing of a ventilation heat exchanger core. As shown in the figure, a 125mm air duct is routed through the ground, beneath the heated floor from the outdoor air into the basement. Ambient air is sucked through the ground into the basement and while traversing the ground, the under floor heat losses is recovered by the ducted air and warm air is then delivered into the unheated basement. A part of the room air is also entrained to the basement because of the suction pressure caused by a blower in a ventilation heat exchanger. This is one of the methods for heating the basement, which has no explicit room heaters. The basement is also partially heated with the heat losses from the water storage tank located in the basement. The warm air in the basement is then led through an air duct embedded in the east-facing wall cavity into the ventilation heat exchanger on the 2F of the building. This technique completely eliminates the problem of freezing moist air on the heat exchanger surfaces even in very cold climate regions such as Kitami (The lowest temperature is often below -25°C.) and this is one of the superiorities of this ventilation system design. Freezing moist air on the heat exchanger surfaces is a severe and frequently-occurring problem during the cold season and usually leads to many households switching off the ventilation system during winter.

The ratio of the recovered floor heat losses to the total floor heat losses is shown in Fig. 5 during a typical day in winter. The figure shows that an average of 37% floor heat losses are recoverable due to the newly developed 'geo-heat exchanger' system.

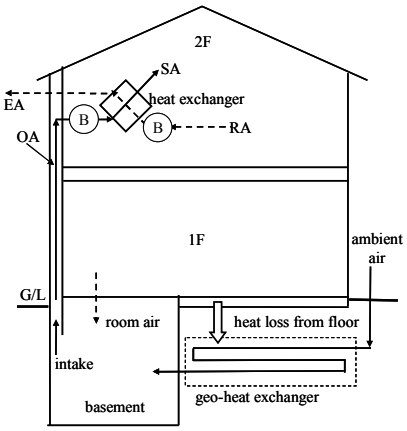

OA: Outdoor Air
SA: Service Air
RA: Room Air
EA: Exhaust Air
B: Blower

Fig. 4 Advanced ventilation system recovers the heat loss from the floor.

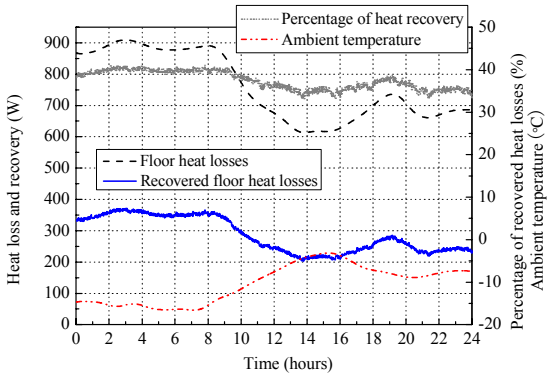

Fig. 5 Percentage of recovered floor heat losses due to enhanced ventilation system.

3.4. Building Heat Transfer

The performance of the system as well as the GHP thermal output depends on the thermal interactions of the building envelope with the surroundings. Detailed building heat transfer modeling was done for Model House in order to determine the total heating load during the winter, spring and autumn seasons and the cooling load during the summer. In modeling the building thermal interactions, radiative, conductive and convective heat exchanges across the walls, windows, floors and roof were computed and accounted for. Across each building component, the *overall thermal resistance* concept was used in evaluating the heat transfer between the indoor and the outdoor through component assemblies. In this concept, the total thermal resistance across a building component assembly (such as a wall assembly) from indoor to the outdoor is the sum of the thermal resistances across the intervening constituent assemblies. Heat transfers arising from ventilation and air leakages around the building envelope were also taken into consideration as well as solar heat gains through the building fenestrations (windows and skylights). Figure 6 shows the computed heat loss profiles for the Model House on typical clear and cloudy days during the winter season. The difference between the profiles of the clear and cloudy days lies in the solar admittance to the building envelope through the fenestrations.

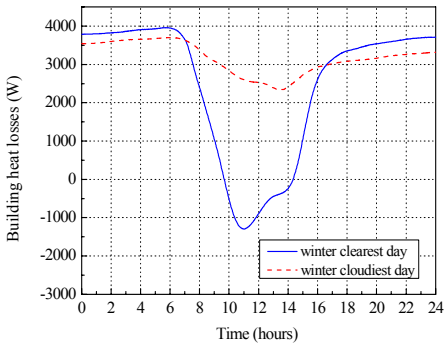

Fig. 6 Computed building heat loss profiles during winter

4. Annual Energy Balances and CO_2 Emissions

An estimation of the annual energy balance (total heat losses from house = thermal demand for room heating) is needed for the evaluations of the system running costs and the Green House Gas (GHG: CO_2) emissions. Details of the annual simulation technique were based on our two previous works [3],[4]. Only two representative days – the clearest and the cloudiest days which are defined by daily energy sum of solar radiations – during each season of the year are used for annual energy balance estimations. Actually measured solar radiation profiles at the Kitami Institute of Technology for 2005 were used for the system simulations and the air temperature data were obtained from the Abashiri Station of the *Automated Meteorological Data Acquisition System* (AMEDAS) in Japan. Wind speed was assumed as 3 m/s (constant) by the data from the AMEDAS. The left bar in Fig. 7 summarizes the results of continuous annual measurements of thermal demand for room

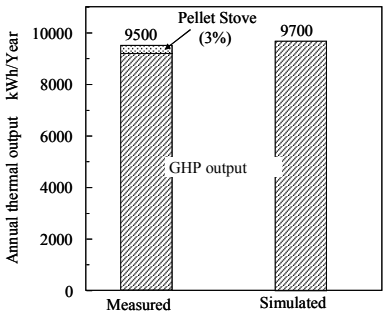

Fig. 7 Annual energy balance in 2005

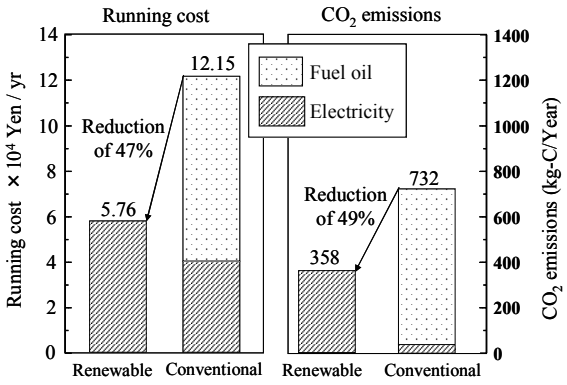

Fig. 8 Improvements of system running cost and CO_2 emissions

heating using a calorimeter mounted on the floor inlet tube during February 2005 ~February 2006. Since the pellet stove was operated for demonstrations in almost all cases, the annual thermal output was only 3 %. The annual average COP (Coefficient of Performance) of the GHP was 2.9. Only 2% deviation of the numerical simulations of the heat losses from actually measured thermal demand was shown in Fig. 7. The figure shows that the annual thermal demand for room heating (= heat loss from house) in 2005 was about 9500 kWh/Year (34.2 GJ/Year). The result showed an important fact that Q-value of 1 W/m^{2}K was realized actually in this house. Figure 8 shows the improvements of the system running cost and GHG (CO_2) emissions in comparison with an equivalent conventional system using numerical simulations for 2005. An equivalent conventional system would have the same building envelope but all the heating demands would be supplied using fuel oil combustion instead of the GHP. Running cost and GHG emissions reductions of 47% and 49% respectively, were obtained for the renewable energy system arising from the use of only the GHP to meet the heating demands of the house.

5. Real-Time System Monitoring and Simulation

5.1 Real-time monitoring

In order to clarify the actual daily performances of the renewable energy system, real-time measurements were carried out on a per-minute basis during the period November 2006 ~ January 2007 using electronic data recorders, hygrometers and temperature gauges. The system parameters that were measured included the floor inlet and outlet temperatures, geothermal tube inlet and return temperatures, room temperatures on the 1F and 2F, the floor average surface temperatures on the *1F* and *2F*, the GHP compressor input power and the thermal output. The continuous measurements and real-time monitoring of these parameters therefore, provided a complete description of the actual performance of the system under actual operating conditions. The block diagram shown in Fig. 9 summarizes the actual operation of the Model House. The set temperature, T_{set} is manually set (a digital display) as the GHP output brine temperature, based on the comfort level of the occupant(s) and this value of T_{set} is then used by the inverter unit to correctly meter out the compressor input power through a controller. For system analysis purposes, the set temperature, T_{set}, was regarded as the system input which determines the steady-state and dynamic responses of the renewable energy system. During measurement activities, various values of T_{set} were implemented in order to evaluate the dynamic and steady-state characteristics of the system.

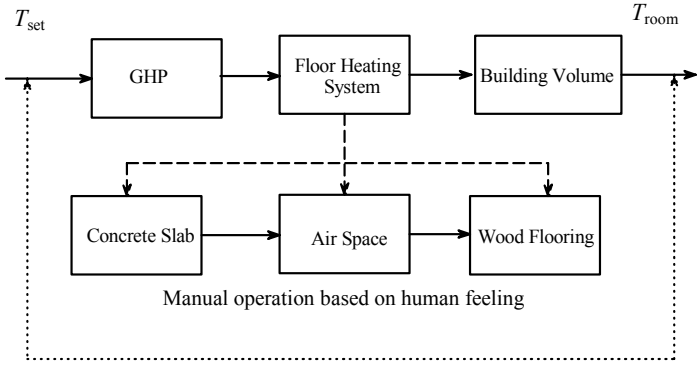

Fig. 9 System operation and energy flows

5.2 System Dynamic Response, Time Constant, and Time Delays

The combined heat flux on the floor heater surface (room-side heat flux), excluding the downward floor heat losses can be determined from the GHP thermal output Q_{GHP} and the effective floor area, A_{floor} according to Eq. (2):

$$q_h = Q_{GHP} / A_{floor} \quad (2)$$

In order to evaluate the average surface temperature of the heated concrete, T_{con}, which governs the room-side heat flux, the following energy balance equations can be written for the floor heating system (Fig. 10):

$$(mc_p)_{con} \frac{dT_{con}}{dt} = q_h - (q_1 + q_2 + q_L) \quad (3)$$

$$(mc_p)_{floor} \frac{dT_{floor}}{dt} = (q_1 + q_2) - (q_3 + q_4) \quad (4)$$

where (mc_p) denotes thermal capacitances per unit floor area and the subscripts *con* and *floor* denote the concrete slab and the wood flooring respectively. q_h is the GHP thermal output (per unit area) and q_L is the downward heat losses of the concrete slab which are normally part of the building heat loss modeling. The fluxes, q_1 and q_3 denote convective heat transfers while q_2 and q_4 denote radiative heat exchanges between the concrete surface and the wood floor, and between the wood floor and the room interior, respectively. The convective and radiative heat fluxes can be estimated using standard methods of heat transfer engineering.

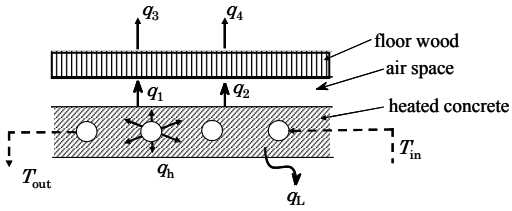

Fig. 10 Energy balance of floor heating system

The GHP system time constant, τ is necessary in order to predict the floor inlet temperature from the GHP which determines the coefficient of performance (*COP*) of the GHP. The *COP* is a function of both the floor heater inlet temperature and the geothermal tube return temperature. Figure 11 is the measured performance curve for the GHP unit itself. Figure 12 shows the dynamic response of the floor heater inlet temperature to a unit step function of T_{set}, with a time constant of about 29.5 minutes. This actually measured time constant τ, also includes the thermal delay introduced by the buffer tanks that are usually attached to the GHP evaporator and condenser units. The profile shown in Fig. 12 was used to dynamically predict the room temperatures due to changes in the set temperature, T_{set}.

The energy transfer between the GHP and the building space is impeded by several time delays introduced by the concrete slab, the intervening air space and the wood flooring that separates the thermal output from the GHP and the living space. In order to account for the components' delays, the Radiant Time Series (RTS) [10] concept was used which takes into account the time delay of both conductive heat gain through opaque massive surfaces like

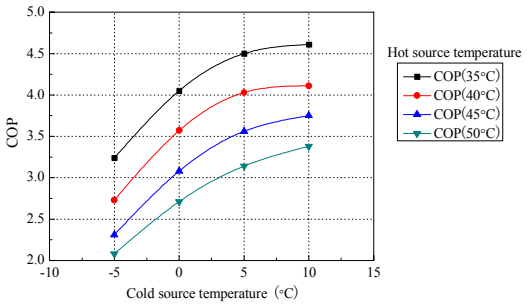

Fig. 11 Variation of COP with the hot-source and cold-source temperatures

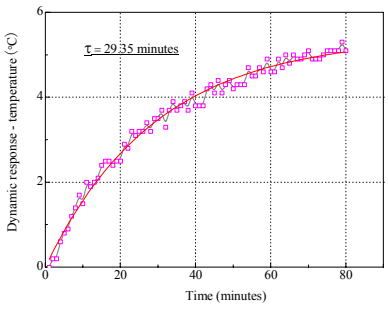

Fig. 12 Dynamic response of the floor inlet temperature to a step change in T_{set}

concretes, woods, etc and the time delay of the radiative heat transfer between the components into the living space. The conductive or radiative heat transfer through any component using the current input and the contribution of past inputs can be written using conductive/radiative time series as follows [10]:

$$q_q = c_0 q_{i,q} + c_1 q_{i,q-1} + c_2 q_{i,q-2} + \ldots + c_n q_{i,q-n} \quad (5)$$

where q_q is the total conductive/radiative heat transfer for the current time (hour or minute), $q_{i,q}$ is the instantaneous contribution to the heat transfer for the current time, $q_{i,q-n}$ is the instantaneous contribution to the current heat transfer, n hours (or minutes) ago, and c_0, c_1, etc are the conductive or radiative time series factors. Full details of this method can be found in Ref. 10.

5.3 Real-time Performances and System Simulation Results

Figures 13 and 15 show the sample results of actual and simulated temperature profiles for January 17 and 18, 2007 respectively. Figures 14 and 16 show the compressor input power, the GHP thermal output and the COP during the two days respectively. For the model house, the GHP operation must be switched off for two hours (4PM ~ 5PM and 6PM ~ 7PM) every day because of the regulations in the contract for the use of the special electricity price menu ('Snow Melting'[4]) for running the GHP unit. These periods of no-operation can be seen in Figs. 14 and 16 but the overall system performance is not at all affected by these temporary shut-downs because of the large thermal capacitance of the floor system (concrete-air space-wood floor system). Thus in Figs. 13 and 15, numerical simulations and actual measurements indicate that the room temperature can still be maintained relatively within the desired range and there is no need for any other auxiliary heating system (the pellet stove), even during the shut-down operations. In particular, Fig. 13 shows the response of the system to a step input during January 17, 2007. At 4:00AM,

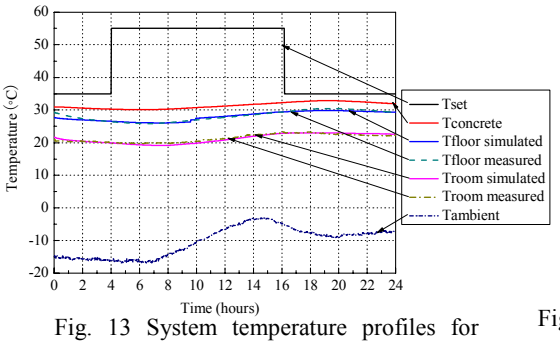

Fig. 13 System temperature profiles for January 17, 2007

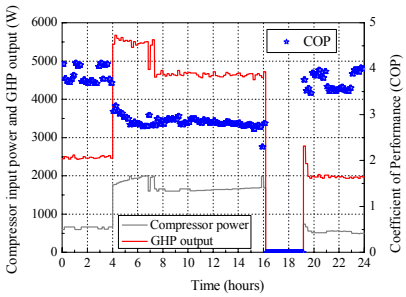

Fig. 14 Compressor input power, GHP thermal output and COP on January 17, 2007

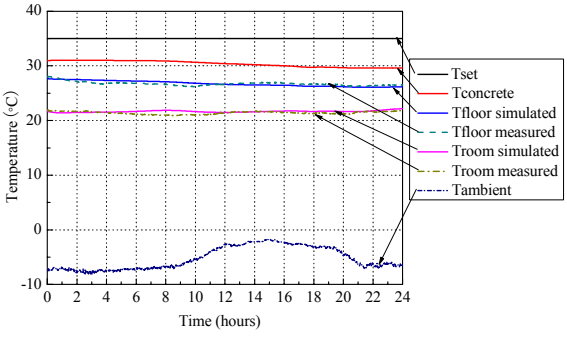

Fig. 15 System temperature profiles for January 18, 2007

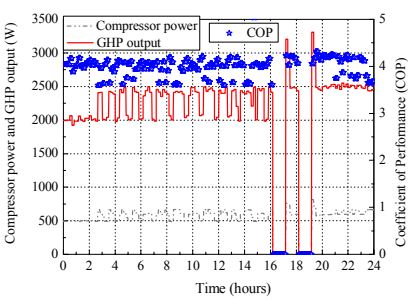

Fig. 16 Compressor input power, GHP thermal output and COP on January 18, 2007

the set temperature, T_{set}, was suddenly increased from 35°C to 55°C manually and the room temperature response was monitored continuously every minute. As shown in Fig. 13, actual measurements and numerical simulations indicate a system delay of about 4 hours for the room temperature change. This may be attributed to the peculiar construction of the floor heating system which comprises the thick (75mm) concrete slab, an intervening air space and the wood finish for the floor covering (Figs. 3 and 10) which introduces time delays for the room-side heat flux .

Figure 17 shows the measured period average GHP thermal output (■) in GJ/day, during various periods spanning November 23, 2006 ~ January 18, 2007. The daily average actually measured ambient temperatures during the periods are also shown and a clear correlation can be established between the relative values of the ambient temperature and the GHP outputs. The building heat loss (=thermal demand) which was obtained through detailed building heat transfer modeling and simulations mentioned above (§ 3) was also shown in figure 17 (○). The building heat loss corresponds to an average building Q_{eq} value of 1.09 W/m^2/K. Since the deviations between the GHP output and building heat loss contained actually surplus (or shortage) heat caused by the delay which was brought to the next period, the better agreement of these, generally, was obtained in the longer averaging period. Averaging of a couple of weeks is sufficient to predict the GHP thermal demand as the building heat loss by quasi-steady treatment (every one minute).

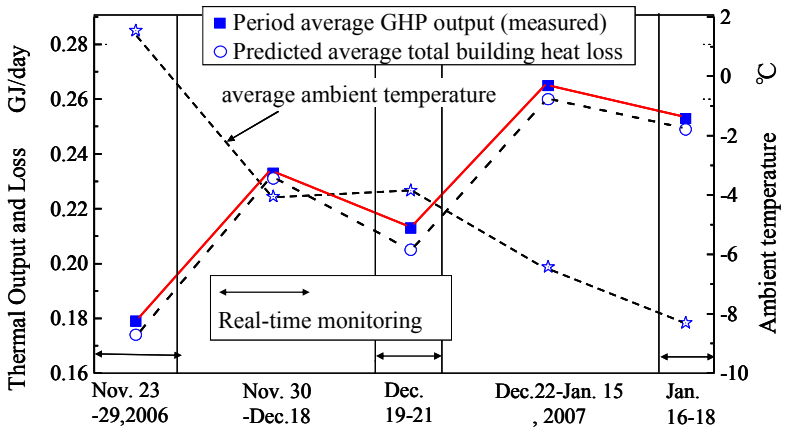

Fig. 17 Comparison of the building thermal demand with GHP thermal output

6. Cost Analysis

Popularization of geothermal heat pump (GHP) in Japan is so far behind the burgeoning activity in northern Europe and North America [11]. It is considered that one of the major reasons is found in the cost disadvantage. The cost analyses reflect only the cost of room heating for a typical residential family of four persons. Table 4 summarizes the initial cost estimations for a GHP-only powered renewable energy system and an equivalent conventional system. The initial cost estimates reflect projected market prices in Japan assuming that both current prices of the GHP components and current cost of the constructions such as excavation will reduce to about a half into the next decade due to continuous popularization of GHP systems with no development of advanced technologies. As a result of these assumptions, the initial cost of the GHP system would be ¥ 2,000,000 (Japanese Yen), while the initial cost of the conventional oil heater system is about ¥200,000 as shown in Table 4. It is assumed that the conventional system uses fuel oil for room heating for the same house configurations, i.e. for the same thermal demand. The

discount price of the electricity of ¥7.518 /kWh was actually applied by the 'Snow Melting' menu [3] of Hokkaido Electric Power Co.. In this contract, the GHP operation must be switched off for two hours every day as mentioned above (§5.3). Figure 18 shows the strong dependence of the 'payback period' on the oil price. If the cost of heating oil keeps increasing from the current value of ¥80/L (litter) up to ¥120/L, then the payback period for a GHP-powered renewable energy system is about 14 years. If 30% of the initial cost of the GHP renewable energy system is funded by the government or some other agencies, this payback period reduces to about 10 years. The greater the availability of funding from relevant agencies due to the popularization of renewable energy systems, the less will be the payback time for any loan or capital taken to set up GHP-only renewable energy systems. Presently, one demerit of renewable energy systems is their very high initial costs but as the popularization and funding of these systems increase through the years, the more attractive these systems will become as reliable alternatives to conventional systems.

Table 4 Projected initial cost estimates for system components

Components		Initial cost estimate (10^4 Japanese Yen)
GHP system	Excavation of GHP U-tube	50/100m
	Tubing and brines	50
	Floor heating construction	50
	GHP unit (1.7kW)	50
	Total	200
Conventional system	Total cost of fan heaters, oil servers, kerosene tank, etc	20

(1 US $ = ¥110 - ¥120)

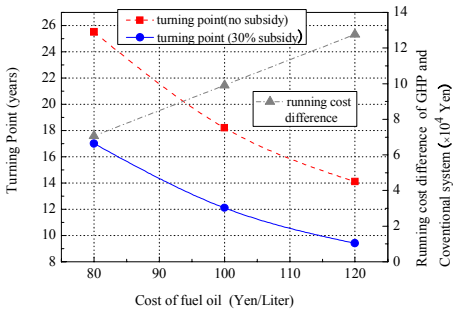

Fig. 18 Payback period for GHP room heating system

7. Conclusions

A detailed study of an actual geothermal heat pump (GHP) powered house equipped with a floor heating system was undertaken. The house is specially configured to suit very cold climate regions, with a well insulated and warm air-jacketed wall and roof assemblies resulting in a Q value of about 1 W/m^{2}K coupled with a well-sealed building with a C-value of about 0.3 cm^2/m^2. Annual daily measurements reveal that only the GHP (1.5kW rating) is entirely sufficient to meet the demands of room heating throughout the year with no need for any auxiliary heating system, even in a very cold location like Kitami city. The large thermal capacitance of the floor heating system (concrete, air space and wood flooring) ensures a very smooth system operation even during periods of mandatory shut-downs due to electricity price menu regulations. An enhanced ventilation system where the outside supply air into the ventilation heat exchanger is first routed through the ground proves to be very effective in recovering the downward heat losses from the floor. This eliminates completely the problem of freezing at the heat exchanger core membranes which is usually a severe ventilation problem in very cold regions, while also recovering part of the floor heat losses. Actual measurements and numerical simulations show that the annual room heating demand for a typical family of four persons is about 9000 ~ 10 000 kWh/Year (33 ~ 36GJ/Year), a greater part of the heating demand recorded during the severe winter season. The use of the GHP results in reductions of about 47% and 49% of the system running costs and GHG (CO_2) emissions respectively, compared to an equivalent conventional system that

uses fuel oil to meet the same heating demand. Cost analysis shows that if the cost of fuel oil in Japan keeps increasing from the current value of ¥80/L up to ¥120/L (50% increase), then the payback period for a GHP-powered renewable energy system is about 14 years. If 30% of the initial cost of the GHP renewable energy system is funded by the government or some other agencies, this payback period reduces to about 10 years.

Acknowledgement

The authors are deeply indebted to President Tsuchiya of Kouei Buildings Co., Kitami for the permission to use the research facility (the Model House) for measurements and observations. We are also grateful to all students at the Energy and Environment Engineering Laboratory in the Kitami Institute of Technology, for cooperation in the measurements at the Model House.

References

(1) IPCC, 2001a Climate Change, United Nations Intergovernmental Panel on Climate Change, Cambridge Press, UK, (2001), Available online at: http://www.ipcc.ch/
(2) N. Endoh, M. Sasaki and K. Doi, Improvement of Thermal Collecting Efficiency of a Photovoltaic/Thermal Hybrid Solar Panel for Cold Climates, *Proceedings of the Intern. Conference on Power Engineering-03 (ICOPE-03)*, 2003
(3) Akpan, I.E., Sasaki, M., and Endoh, N. Simplifications of Simulation on Energy Balances and Estimations of a Hybrid Renewable Energy System for use in Cold Climate Regions, *JSME International Journal, Series B*, Vol. 49, No. 3, (2006), pp. 839-846.
(4) Akpan, I.E., Sasaki, M., and Endoh, N. Optimization of Domestic-size Renewable Energy System Designs Suitable for Cold Climate Regions, *JSME International Journal, Series B*, Vol. 49, No. 4, (2006), pp. 1241-1252.
(5) ASHRAE Handbook, *HVAC Systems and Equipment* (SI Edition), ASHRAE Inc., Atlanta, (2004), pp. 6.1.
(6) Sattari, S., and Farhanieh, B., A Parametric Study on Radiant Floor Heating System Performance, *Renewable Energy*, Vol. 31 (2006), pp. 1617-1626.
(7) Weitmann, P., Kragh, J., Roots, P., and Svendsen, S., Modeling Floor Heating Systems Using a Validated Two-Dimensional Ground-Coupled Numerical Model, *Building and Environment*, Vol. 40 (2005), pp. 153-163.
(8) Zaheer-Uddin, M., Zheng, G. R., and Cho, S., Optimal Operation of Embedded-Piping Floor Heating System with Control Input Constraints, *Energy Convers. Mgmt*, Vol. 38, No. 7 (1997), pp. 713-725.
(9) Alkhalaileh, M. T., Atieh, K. A., Nasser, N. G., and Jubran, B. A., Modelling and Simulation of Solar Pond Floor Heating System, *Renewable Energy*, Vol. 18 (1999), pp. 1-14.
(10) ASHRAE Handbook, *Fundamentals* (SI Edition), ASHRAE Inc., Atlanta, (2005), pp. 31.47.
(11) Lund, J. et al, Geothermal (Ground-source) Heat Pumps a World Overview, *GHC Bulletin*, (2004), pp.1-10.